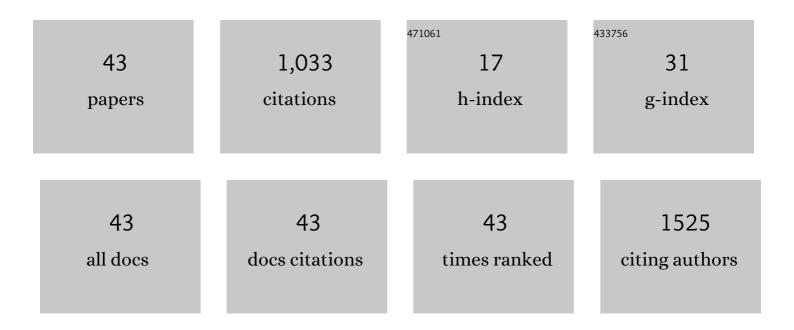
Guido Buonincontri

List of Publications by Year in descending order

Source: https://exaly.com/author-pdf/6408617/publications.pdf Version: 2024-02-01



#	Article	IF	CITATIONS
1	Simultaneous relaxometry and morphometry of human brain structures with 3D magnetic resonance fingerprinting: a multicenter, multiplatform, multifield-strength study. Cerebral Cortex, 2023, 33, 729-739.	1.6	4
2	Learning residual motion correction for fast and robust 3D multiparametric MRI. Medical Image Analysis, 2022, 77, 102387.	7.0	7
3	Repeatability and reproducibility of human brain morphometry using threeâ€dimensional magnetic resonance fingerprinting. Human Brain Mapping, 2021, 42, 275-285.	1.9	13
4	Three dimensional MRF obtains highly repeatable and reproducible multi-parametric estimations in the healthy human brain at 1.5T and 3T. NeuroImage, 2021, 226, 117573.	2.1	26
5	Accelerated 3D whole-brain T1, T2, and proton density mapping: feasibility for clinical glioma MR imaging. Neuroradiology, 2021, 63, 1831-1851.	1.1	15
6	Quantitative imaging metrics derived from magnetic resonance fingerprinting using ISMRM/NIST MRI system phantom: An international multicenter repeatability and reproducibility study. Medical Physics, 2021, 48, 2438-2447.	1.6	20
7	Compressive MRI quantification using convex spatiotemporal priors and deep encoder-decoder networks. Medical Image Analysis, 2021, 69, 101945.	7.0	15
8	Pattern-Matching Unit for Medical Applications. IEEE Transactions on Nuclear Science, 2021, 68, 2140-2145.	1.2	0
9	Accuracy and repeatability of QRAPMASTER and MRF-vFA. Magnetic Resonance Imaging, 2021, 83, 196-207.	1.0	6
10	Magnetic resonance fingerprinting of the pancreas at 1.5ÂT and 3.0ÂT. Scientific Reports, 2020, 10, 17563.	1.6	12
11	Rapid three-dimensional multiparametric MRI with quantitative transient-state imaging. Scientific Reports, 2020, 10, 13769.	1.6	29
12	Retrospective rigid motion correction of threeâ€dimensional magnetic resonance fingerprinting of the human brain. Magnetic Resonance in Medicine, 2020, 84, 2606-2615.	1.9	23
13	Fast Quantitative Magnetic Resonance Imaging. Synthesis Lectures on Biomedical Engineering, 2020, 15, i-124.	0.1	Ο
14	Designing contrasts for rapid, simultaneous parameter quantification and flow visualization with quantitative transient-state imaging. Scientific Reports, 2019, 9, 8468.	1.6	15
15	A novel cyclic biased agonist of the apelin receptor, MM07, is disease modifying in the rat monocrotaline model of pulmonary arterial hypertension. British Journal of Pharmacology, 2019, 176, 1206-1221.	2.7	32
16	Flexible and efficient optimization of quantitative sequences using automatic differentiation of Bloch simulations. Magnetic Resonance in Medicine, 2019, 82, 1438-1451.	1.9	24
17	Feasibility of Quantitative Magnetic Resonance Fingerprinting in Ovarian Tumors for T ₁ and T ₂ Mapping in a PET/MR Setting. IEEE Transactions on Radiation and Plasma Medical Sciences, 2019, 3, 509-515.	2.7	13
18	An Aristotelian View on MR-Based Attenuation Correction (ARISTOMRAC): Combining the Four Elements. IEEE Transactions on Radiation and Plasma Medical Sciences, 2019, 3, 491-497.	2.7	3

GUIDO BUONINCONTRI

#	Article	IF	CITATIONS
19	Multi-site repeatability and reproducibility of MR fingerprinting of the healthy brain at 1.5 and 3.0â€⊤. NeuroImage, 2019, 195, 362-372.	2.1	67
20	Magnetic resonance fingerprinting with dictionaryâ€based fat and water separation (DBFW MRF): A multiâ€component approach. Magnetic Resonance in Medicine, 2019, 81, 3032-3045.	1.9	39
21	Silent T ₂ [*] and T ₂ encoding using ZTE combined with BURST. Magnetic Resonance in Medicine, 2019, 81, 2277-2287.	1.9	8
22	Monoamine oxidase-dependent endoplasmic reticulum-mitochondria dysfunction and mast cell degranulation lead to adverse cardiac remodeling in diabetes. Cell Death and Differentiation, 2018, 25, 1671-1685.	5.0	54
23	Elabela/Toddler Is an Endogenous Agonist of the Apelin APJ Receptor in the Adult Cardiovascular System, and Exogenous Administration of the Peptide Compensates for the Downregulation of Its Expression in Pulmonary Arterial Hypertension. Circulation, 2017, 135, 1160-1173.	1.6	183
24	Spiral MR fingerprinting at 7 T with simultaneous B1 estimation. Magnetic Resonance Imaging, 2017, 41, 1-6.	1.0	37
25	MR fingerprinting with simultaneous B1 estimation. Magnetic Resonance in Medicine, 2016, 76, 1127-1135.	1.9	124
26	Direct Evaluation of MR-Derived Attenuation Correction Maps for PET/MR of the Mouse Myocardium. IEEE Transactions on Nuclear Science, 2016, 63, 195-202.	1.2	1
27	Impaired Limbic Cortico-Striatal Structure and Sustained Visual Attention in a Rodent Model of Schizophrenia. International Journal of Neuropsychopharmacology, 2015, 18, pyu010-pyu010.	1.0	28
28	Combining MRI With PET for Partial Volume Correction Improves Image-Derived Input Functions in Mice. IEEE Transactions on Nuclear Science, 2015, 62, 628-633.	1.2	3
29	Complex I Deficiency Due to Selective Loss of Ndufs4 in the Mouse Heart Results in Severe Hypertrophic Cardiomyopathy. PLoS ONE, 2014, 9, e94157.	1.1	41
30	Right Ventricular Dysfunction in the R6/2 Transgenic Mouse Model of Huntington's Disease is Unmasked by Dobutamine. Journal of Huntington's Disease, 2014, 3, 25-32.	0.9	17
31	Functional assessment of the mouse heart by MRI with a 1-min acquisition. NMR in Biomedicine, 2014, 27, 733-737.	1.6	10
32	Trajectory correction for free-breathing radial cine MRI. Magnetic Resonance Imaging, 2014, 32, 961-964.	1.0	11
33	Comparison of first pass bolus AIFs extracted from sequential 18F-FDG PET and DSC-MRI of mice. Nuclear Instruments and Methods in Physics Research, Section A: Accelerators, Spectrometers, Detectors and Associated Equipment, 2014, 734, 137-140.	0.7	3
34	Mitochondria selective S â€nitrosation by mitochondriaâ€targeted S â€nitrosothiol protects against postâ€infarct heart failure in mouse hearts. European Journal of Heart Failure, 2014, 16, 712-717.	2.9	39
35	Combining MRI with PET for partial volume correction improves image-derived input functions in mice. EJNMMI Physics, 2014, 1, A84.	1.3	1
36	PET/MRI assessment of the infarcted mouse heart. Nuclear Instruments and Methods in Physics Research, Section A: Accelerators, Spectrometers, Detectors and Associated Equipment, 2014, 734, 152-155.	0.7	6

#	Article	IF	CITATIONS
37	Quadrature birdcage coil with distributed capacitors for 7.0 T magnetic resonance data acquisition of small animals. Concepts in Magnetic Resonance Part B, 2014, 44, 83-88.	0.3	7
38	PET/MRI in the infarcted mouse heart with the Cambridge split magnet. Nuclear Instruments and Methods in Physics Research, Section A: Accelerators, Spectrometers, Detectors and Associated Equipment, 2013, 702, 47-49.	0.7	6
39	A fast protocol for infarct quantification in mice. Journal of Magnetic Resonance Imaging, 2013, 38, 468-473.	1.9	12
40	MRI and PET in Mouse Models of Myocardial Infarction. Journal of Visualized Experiments, 2013, , e50806.	0.2	8
41	Riociguat Reduces Infarct Size and Post-Infarct Heart Failure in Mouse Hearts: Insights from MRI/PET Imaging. PLoS ONE, 2013, 8, e83910.	1.1	36
42	Direct Evidence of Progressive Cardiac Dysfunction in a Transgenic Mouse Model of Huntington's Disease. Journal of Huntington's Disease, 2012, 1, 57-64.	0.9	31
43	RF coil design for low and high field MRI: Numerical methods and measurements. , 2011, , .		4